Dispersive optical bistability for large photon numbers and low cavity damping

K. Vogel and H. Risken
Abteilung für Theoretische Physik, Universität Ulm, D-7900 Ulm, Federal Republic of Germany
(Received 21 November 1989)

For a quantum-mechanical model of dispersive optical bistability we derive in the classical limit, i.e., for large photon numbers, a two-variable Fokker-Planck equation. For low cavity damping this Fokker-Planck equation can be approximated by a one-variable Fokker-Planck equation which is solved numerically. If, in addition, the number of thermal photons is small compared with the number of photons inside the cavity, an analytical result for the transition rate is obtained.

I. INTRODUCTION

One of the main models in the theory of dispersive optical bistability is the one of Drummond and Walls.[1] In this model a single quantized field mode inside a cavity is driven by an external classical coherent driving field. The nonlinear medium inside the cavity is described by a nonlinear polarization. Dissipation due to cavity losses is taken into account by a coupling to a heat bath. In order to calculate the transition rates between the two bistable states, the equation of motion for the density operator of the system has to be solved. In two publications[2,3] we have solved this equation by transforming it into a c-number equation for the quasiprobabilities of Cahill and Glauber.[4] It turns out that this equation is a partial differential equation for two variables, similar to a Fokker-Planck equation. Generally it contains third-order derivative terms and has a nonpositive definite diffusion matrix. By using the matrix continued-fraction method we have managed to determine the lowest nonzero eigenvalue of this equation, which describes the transition rate between the two stable states of the system.

In the limit of large photon numbers, the equation of motion for the quasiprobability distributions reduces to an ordinary Fokker-Planck equation. Because this Fokker-Planck equation has two variables and detailed balance is not fulfilled, it cannot be solved analytically. The same matrix continued-fraction procedure, that was applied to the exact equation for the quasiprobability distributions, can be used for this Fokker-Planck equation. For small cavity damping an energylike variable becomes a slow variable. Therefore it is possible to eliminate the fast variable and thus transform the two-variable Fokker-Planck equation to an equation with only one variable. Similarly as done for the Brownian motion problem in a bistable potential[5] the lowest nonzero eigenvalue can thus be obtained from this one-variable Fokker-Planck equation for large photon numbers and low cavity damping. The Fokker-Planck equation is, however, quite complicated. The drift and diffusion coefficients are expressed in terms of complete elliptic integrals. Nevertheless, the lowest nonzero eigenvalue can be calculated numerically. If, in addition to the limits described above, the number of thermal photons is small compared with the number of photons inside the cavity, the lowest nonzero eigenvalue can be calculated analytically.

If the cavity losses are small and the number of photons is not too large one can use an alternative method. The nondiagonal elements of the density-matrix equation can be neglected and the resulting equation can be solved directly as is done in Refs. 6 and 7. The work of the present paper (see also Chap. 13 of Ref. 8) is related to the work of Dykman and Smelyanskii,[9] who investigated transitions between stable states of a driven nonlinear oscillator. The work of Haug, Koch, Neumann, and Schmidt[10] should also be mentioned. They solved a Fokker-Planck equation similar to our classical two-variable Fokker-Planck equation by using a matrix continued-fraction method. They have obtained a stationary distribution, but did not calculate transition rates. Graham and Schenzle[11] investigated this equation by some approximation methods. Drummond[12] used adiabatic elimination to obtain a one-dimensional representation-free Fokker-Planck equation which can describe tunneling in absorptive optical bistability near the turning points of the state equation. Filipowicz, Garrison, Meystre, and Wright[13] investigated noise-induced switching in a purely dispersive Kerr medium by solving a first-passage-time problem for a colored noise model.

The present paper is organized as follows. In Sec. II we derive a classical Fokker-Planck equation from the quantum-mechanical equations and discuss it. In Sec. III we assume small cavity damping and approximate the two-dimensional Fokker-Planck equation by a one-dimensional Fokker-Planck equation. In Sec. IV the quantities occurring in this one-dimensional equation are calculated and expressed by complete elliptic integrals. In Sec. V the algorithm for solving the one-dimensional equation is described. In Sec. VI we derive an analytical result for the transition rate, which is valid if the number of thermal photons is small compared to the number of photons inside the cavity. In Sec. VII the numerical and analytical results are presented and compared with each other. Section VIII, finally, gives a brief summary.

II. DERIVATION OF CLASSICAL EQUATIONS

For the model of Drummond and Walls[1] describing dispersive optical bistability the equation of motion for the density operator ρ in a reference frame rotating with the frequency of the external driving field reads

$$\dot{\rho}=-i[H/\hbar,\rho]+\kappa L_{ir}[\rho] , \tag{2.1}$$

where $H/\hbar$ and $L_{ir}[\rho]$ are given by

$$H/\hbar=-\Omega a^{\dagger}a+\chi(a^{\dagger})^2a^2-F(a+a^{\dagger}),\quad \Omega=\omega_L-\omega_c \tag{2.2}$$

$$L_{ir}[\rho]=2a\rho a^{\dagger}-\rho a^{\dagger}a-a^{\dagger}a\rho+2n_{\rm th}[[a,\rho],a^{\dagger}] , \tag{2.3}$$

(see Refs. 1–3). The parameters are defined as follows: χ is the anharmonicity parameter, F is the amplitude of the driving field in proper units, Ω is the difference between the frequency of the driving field and the resonance frequency of the cavity, κ is the cavity damping constant, and $n_{\rm th}$ is the number of thermal photons inside the cavity.

The equation of motion for the density operator can be transformed into a c-number equation by using the quasiprobability distributions of Cahill and Glauber.[4] These quasiprobability distributions, denoted by $W(\alpha,\alpha^*,s)$, can be defined as Fourier transforms of the characteristic functions

$$\chi(\xi,\xi^*,s)=\mathrm{Tr}\{\rho\exp[\xi a^{\dagger}-\xi^*a+(s/2)|\xi|^2]\} , \tag{2.4}$$

i.e., we have

$$W(\alpha,\alpha^*,s)=\frac{1}{\pi^2}\int\chi(\xi,\xi^*,s)e^{\alpha\xi^*-\alpha^*\xi}d^2\xi . \tag{2.5}$$

In Ref. 3 we have shown that the equation of motion for $W(\alpha,\alpha^*,t,s)$ reads

$$\begin{aligned}\frac{\partial W(\alpha,\alpha^*,s,t)}{\partial t}=&\left[-\frac{\partial}{\partial\alpha}[-\kappa\alpha+i\Omega\alpha-2i\chi\alpha^*\alpha^2+2i\chi(1-s)\alpha+iF]\right.\\&-\frac{\partial}{\partial\alpha^*}[-\kappa\alpha^*-i\Omega\alpha^*+2i\chi\alpha\alpha^{*2}-2i\chi(1-s)\alpha^*-iF]+i\chi s\left[\frac{\partial^2}{\partial\alpha^{*2}}\alpha^{*2}-\frac{\partial^2}{\partial\alpha^2}\alpha^2\right]\\&\left.+\kappa(2n_{\rm th}+1-s)\frac{\partial^2}{\partial\alpha^*\partial\alpha}+i\frac{\chi}{2}(1-s^2)\frac{\partial^2}{\partial\alpha^*\partial\alpha}\left[\frac{\partial}{\partial\alpha^*}\alpha^*-\frac{\partial}{\partial\alpha}\alpha\right]\right]W(\alpha,\alpha^*,s,t) .\end{aligned} \tag{2.6}$$

The quasiprobability distribution $W(\alpha,\alpha^*,s,t)$ is characterized by the parameter s. For $s=1$, we have the Glauber-Sudarshan P function, for $s=0$ the Wigner function, and for $s=-1$ the Q function.

From (2.6) we will derive a Fokker-Planck equation for large photon numbers, i.e., for the classical limit. First we introduce the normalized variables

$$z=\sqrt{\chi/\Omega}\alpha,\quad \tilde{t}=\Omega t,\quad \tilde{F}=\sqrt{\chi/\Omega}(F/\Omega),\quad \gamma=\kappa/\Omega \tag{2.7}$$

and transform (2.6) to these variables. In the bistable region the normalized variables z and $\tilde{F}$ are of the order 1; see Ref. 2. In order to obtain a classical Fokker-Planck equation the photon numbers must be large, i.e.,

$$|\alpha|^2=\sqrt{\Omega/\chi}|z|^2\gg 1 \tag{2.8}$$

and

$$n_{\rm th}=\left[\exp\left[\frac{\hbar\omega_c}{kT}\right]-1\right]^{-1}\gg 1 . \tag{2.9}$$

Therefore a classical Fokker-Planck equation can be obtained for

$$\frac{\chi}{\Omega}\ll 1,\quad \frac{\hbar\omega_c}{kT}\ll 1 . \tag{2.10}$$

In this limit we have

$$(2n_{\rm th}+1-s)\frac{\chi}{\Omega}\to\frac{2\chi kT}{\Omega\hbar\omega_c} \tag{2.11}$$

and the quasiprobability distribution becomes a true probability distribution independent of the parameter s. Using (2.10) and (2.11) we obtain the classical Fokker-Planck equation

$$\begin{aligned}\frac{\partial W(z,z^*,\tilde{t})}{\partial\tilde{t}}=&-\frac{\partial}{\partial z}(-\gamma z+iz-2iz^*z^2+i\tilde{F})W(z,z^*,\tilde{t})-\frac{\partial}{\partial z^*}[-\gamma z^*-iz^*+2i(z^*)^2z-i\tilde{F}]W(z,z^*,\tilde{t})\\&+4\gamma\Theta\frac{\partial^2W(z,z^*,\tilde{t})}{\partial z\,\partial z^*} ,\end{aligned} \tag{2.12}$$

where the normalized temperature Θ is given by

$$\Theta=\frac{1}{2}\frac{\chi}{\Omega}\frac{kT}{\hbar\omega_c} . \tag{2.13}$$

Because in our further calculations only normalized quantities occur the tilde in $\tilde{t}$ and $\tilde{F}$ will be omitted. In real nota-

tion, i.e., $z=x+iy$, (2.12) can then be written as

$$\frac{\partial W(x,y,t)}{\partial t}=-\frac{\partial}{\partial x}[-\gamma x-y+2(x^2+y^2)y]W(x,y,t)-\frac{\partial}{\partial y}[-\gamma y+x-2(x^2+y^2)x+F]W(x,y,t)$$
$$+\gamma\Theta\left[\frac{\partial^2}{\partial x^2}+\frac{\partial^2}{\partial y^2}\right]W(x,y,t)\ . \tag{2.14}$$

Equations (2.12) and (2.14) are indeed Fokker-Planck equations because the diffusion matrix is clearly positive definite. As already pointed out in Ref. 3 (2.6) has the form of a Fokker-Planck equation for $s=\pm 1$. The diffusion matrix of this Fokker-Planck-like equation is, however, not positive definite or positive semidefinite.

The Langevin equations corresponding to the Fokker-Planck equation (2.14) read

$$\begin{aligned}\dot{x}&=-\gamma x-y+2(x^2+y^2)y+\Gamma_x(t)\ ,\\ \dot{y}&=-\gamma y+x-2(x^2+y^2)x+F+\Gamma_y(t)\ ,\end{aligned} \tag{2.15}$$

where the Langevin forces $\Gamma_x(t)$ and $\Gamma_y(t)$ are Gaussian white noise forces with the following expectation values:

$$\begin{aligned}&\langle\Gamma_x(t)\rangle=\langle\Gamma_y(t)\rangle=\langle\Gamma_x(t)\Gamma_y(t')\rangle=0\ ,\\ &\langle\Gamma_x(t)\Gamma_x(t')\rangle=\langle\Gamma_y(t)\Gamma_y(t')\rangle=2\gamma\Theta\delta(t-t')\ .\end{aligned} \tag{2.16}$$

It is worthwhile noticing that (2.14) and (2.15) are the Fokker-Planck and Langevin equations for a driven Duffing oscillator[14,15] in the rotating-wave approximation with the additive noise; see, for instance, Sec. II B of Ref. 2. It can easily be shown that the undamped system (i.e., $\gamma=0$ and no Langevin forces) can be described by the following Hamiltonian equations:

$$\dot{x}=\frac{\partial H}{\partial y}\ ,\quad \dot{y}=-\frac{\partial H}{\partial x}\ , \tag{2.17}$$

where the Hamilton function H is given by

$$H=\tfrac{1}{2}(x^2+y^2)-\tfrac{1}{2}(x^2+y^2)-Fx\ . \tag{2.18}$$

Because the Hamilton function is time independent, $H(x,y)$ is a constant of motion and the trajectories of (2.17) are given by $H(x,y)=E$. The x axis is a symmetry axis for the trajectories. They cross the x axis at x_0, where x_0 follows from $H(x_0,y=0)=E$.

For a discussion of the undamped motion it is useful to have a closer look at the function

$$f(x)=H(x,y=0)=\tfrac{1}{2}x^4-\tfrac{1}{2}x^2-Fx\ . \tag{2.19}$$

For $0\le|F|<2/(3\sqrt{6})$, $f(x)$ has two minima and one maximum; see Fig. 1(a). The energies corresponding to these extrema are E_0, E_c, and E_1 as indicated in Fig. 1(a). For $E_0<E<E_c$, $f(x)=E$ has two real solutions and there is only one trajectory $H(x,y)=E$. For $E_c<E<E_1$, $f(x)=E$ has four real solutions and we have two trajectories $H(x,y)=E$. For $E>E_1$, finally, $f(x)=E$ has only two real solutions and there is only one trajectory $H(x,y)=E$. Some trajectories for various energy values are shown in Fig. 1(b).

For $|F|>2/(3\sqrt{6})$, $f(x)$ has one minimum and there is only one trajectory $H(x,y)=E$ for any energy value above the minimum energy E_0; see Fig. 2(a). Figure 2(b) shows some trajectories for $|F|>2/(3\sqrt{6})$. This case will not be investigated further because we are interested in bistability. If the system is damped, i.e., $\gamma\neq 0$, and if no Langevin forces are present, we have the following stationary solutions:

$$x=\frac{(2I-1)F}{\gamma^2+(2I-1)^2}\ ,\quad y=\frac{\gamma F}{\gamma^2+(2I-1)^2}\ , \tag{2.20}$$

where I is defined by

$$I=x^2+y^2\ , \tag{2.21}$$

which in turn is determined by

$$F^2=I[\gamma^2+(2I-1)^2]\ . \tag{2.22}$$

Note that, in contrast to a damped motion of a particle in a potential, these stationary solutions depend on the damping constant.

For small damping the stationary solutions are in the vicinity of the points determined by

$$\frac{\partial H}{\partial x}=\frac{\partial H}{\partial y}=0\ . \tag{2.23}$$

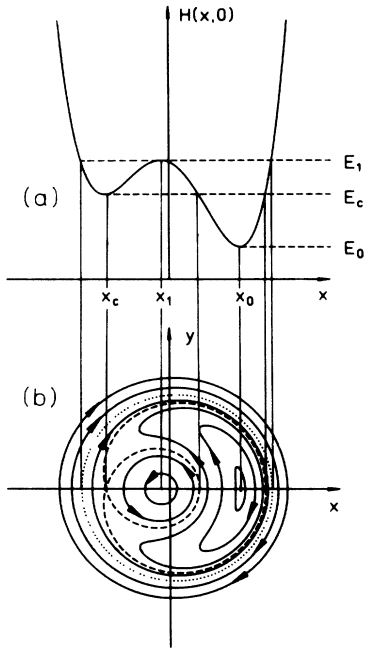

FIG. 1. The function (a) $f(x)=H(x,0)$ and some trajectories (b) $H(x,y)=E$ for $|F|<2/(3\sqrt{6})$. The trajectory $H(x,y)=E_c$ is shown by a dashed line, the trajectory $H(x,y)=E_1$ by a dotted line.

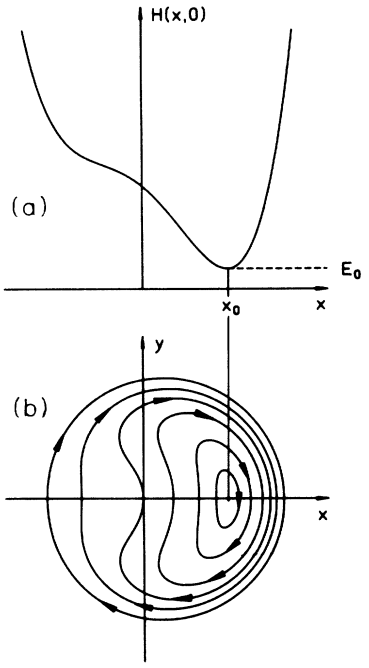

FIG. 2. The function (a) $f(x)=H(x,0)$ and some trajectories (b) $H(x,y)=E$ for $|F|>2/(3\sqrt{6})$.

A linearization procedure shows that the stationary solutions, which are close to the minimum or maximum of H, are stable and that the stationary solution, which is near the saddle point of H, is unstable. (In the Brownian motion problem the Hamilton function can only have minima and saddle points because the kinetic energy is always positive. The minima are stable and the saddle points are unstable if the system is damped.) In the zero-friction limit, the system described by (2.15) is bistable for $F<2/(3\sqrt{6})$ (for these F values H has one minimum, one maximum, and one saddle point). For $F>2/(3\sqrt{6})$, H has only one minimum, i.e., there is only one (stable) stationary solution. For finite damping the region of F values, where bistability exists, is changed; see (2.20) and Sec. II A of Ref. 2.

III. TRANSFORMATION OF THE FOKKER-PLANCK EQUATION AND ELIMINATION OF THE FAST VARIABLE

For the undamped system the energy is a constant of motion. For small damping it is a slowly varying variable because the energy loss due to the damping terms as well as the correlation function of the Langevin forces scale with γ. Therefore we introduce the energy E as a new variable. As a second variable we use the time τ which the solution $x(t),y(t)$ of the Hamilton equation (2.17) [i.e., the equation of motion (2.15) with no damping forces and no Langevin forces] needs to go from a given starting point (x_0,y_0) to the point (x,y) along the trajectory $H(x,y)=E$. Obviously the trajectory crosses the x axis at two points. As starting point we choose the one with the larger x coordinate. This means that we describe an arbitrary point (x,y) by the energy E, which tells us which trajectory we are on, and by the traveling time τ, which tells us where we are on this trajectory.

Because there are two trajectories $H(x,y)=E$ for $E_c<E<E_1$ we divide the x-y plane into three regions as indicated in Fig. 3. These three regions are characterized as follows:

I: $E_0<E<E_c$, only one trajectory

II: $E_c<E<E_1$, the inner of the two trajectories

IIIa: $E_c<E<E_1$, the outer of the two trajectories

IIIb: $E_1<E$, only one trajectory .

IV: $E_1<E$, only one trajectory .

At $E=E_1$ nothing special happens in region III. Only the inner trajectory $H(x,y)=E$ (region II) ceases to exist and the energy E uniquely determines the trajectory for $E>E_1$.

A transformation of the Fokker-Planck equation (2.14) to the new variables τ and E yields for regions I–III

$$\frac{\partial\tilde{W}}{\partial t}=-\frac{\partial}{\partial E}D_E\tilde{W}-\frac{\partial}{\partial\tau}D_\tau\tilde{W}+\frac{\partial^2}{\partial E^2}D_{EE}\tilde{W}+2\frac{\partial^2}{\partial\tau\,\partial E}D_{\tau E}\tilde{W}+\frac{\partial^2}{\partial\tau^2}D_{\tau\tau}\tilde{W}\ . \tag{3.1}$$

For our further calculations we do not need D_τ, $D_{\tau E}$, and $D_{\tau\tau}$. Therefore we give only the result for D_E and D_{EE}:

$$D_E=-\gamma\left[\frac{\partial H}{\partial x}x+\frac{\partial H}{\partial y}y\right]+\gamma\Theta\left[\frac{\partial^2 H}{\partial x^2}+\frac{\partial^2 H}{\partial y^2}\right], \tag{3.2a}$$

$$D_{EE}=\gamma\Theta\left[\left[\frac{\partial H}{\partial x}\right]^2+\left[\frac{\partial H}{\partial y}\right]^2\right]. \tag{3.2b}$$

Because the Jacobian of the transformation is equal to 1, i.e.,

$$J=\left|\frac{\partial(x,y)}{\partial(\tau,E)}\right|=\frac{\partial x}{\partial\tau}\frac{\partial y}{\partial E}-\frac{\partial y}{\partial\tau}\frac{\partial x}{\partial E}=\frac{\partial H}{\partial y}\frac{\partial y}{\partial E}+\frac{\partial H}{\partial x}\frac{\partial x}{\partial E}=1\ , \tag{3.3}$$

we have

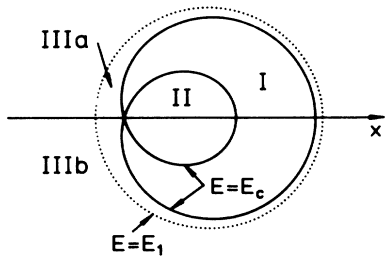

FIG. 3. The trajectory $H(x,y)=E_c$, which divides the x-y plane into three different regions.

$$W(x,y)dx\,dy=\tilde{W}(\tau,E)d\tau\,dE=\tilde{W}(\tau,E)dx\,dy\ . \tag{3.4}$$

Until now we have not used the fact that E is a slowly varying variable for small damping. If γ is small, the solution of (2.15) will make many round trips along the trajectory $H(x,y)=E$ until it is removed appreciably from the trajectory by the damping forces or by the Langevin forces. The essential approximation for small damping is that $\tilde{W}(\tau,E)$ is almost independent of τ. The probability distribution for the energy E, denoted by $\hat{W}(E)$, is then given by

$$\hat{W}(E)=\int_0^{T(E)}\tilde{W}(\tau,E)d\tau=T(E)W(E)\ . \tag{3.5}$$

For our further calculations we do not use $\hat{W}(E)$ but $W(E)$; see also Refs. 5 and 16. Integration of (3.1) with respect to τ, i.e., calculating integrals of the form

$$\int_0^{T(E)}\cdots d\tau\ , \tag{3.6}$$

then yields

$$T(E)\frac{\partial W(E,t)}{\partial t}=-\frac{\partial}{\partial E}\left[\int_0^{T(E)}D_E(\tau,E)d\tau\right]W(E,t)+\frac{\partial^2}{\partial E^2}\left[\int_0^{T(E)}D_{EE}(\tau,E)d\tau\right]W(E,t)\ . \tag{3.7}$$

The other terms cancel because $D_\tau(\tau,E)$, $D_{\tau E}(\tau,E)$, and $D_{\tau\tau}(\tau,E)$ are periodic in τ. (It follows from the definition of τ that all unique functions in the x-y plane are periodic in τ.)

By using Stokes's theorem one can show the following identity:

$$\frac{\partial}{\partial E}\int_0^{T(E)}\left[\left[\frac{\partial H}{\partial x}\right]^2+\left[\frac{\partial H}{\partial y}\right]^2\right]d\tau=\int_0^{T(E)}\left[\frac{\partial^2 H}{\partial x^2}+\frac{\partial^2 H}{\partial y^2}\right]d\tau\ . \tag{3.8}$$

Substituting this result into (3.7) leads to

$$T(E)\frac{\partial W(E,t)}{\partial t}=2\gamma\frac{\partial}{\partial E}\left[I(E)+\Theta J(E)\frac{\partial}{\partial E}\right]W(E,t) \tag{3.9}$$

as the final form of our one-dimensional Fokker-Planck equation. For each of the regions I–III the functions $I(E)$ and $J(E)$ occurring in (3.9) are given by

$$I(E)=\tfrac{1}{2}\int_0^{T(E)}\left[\frac{\partial H}{\partial x}x+\frac{\partial H}{\partial y}y\right]d\tau=\mp\int dx\,dy\ , \tag{3.10a}$$

$$J(E)=\tfrac{1}{2}\int_0^{T(E)}\left[\left[\frac{\partial H}{\partial x}\right]^2+\left[\frac{\partial H}{\partial y}\right]^2\right]d\tau=\mp\tfrac{1}{2}\int\left[\frac{\partial^2 H}{\partial x^2}+\frac{\partial^2 H}{\partial y^2}\right]dx\,dy\ . \tag{3.10b}$$

The integrals $\int\cdots d\tau$ are calculated along the trajectory $H(x,y)=E$, whereas the integrals $\int\cdots dx\,dy$ are calculated over the area enclosed by this trajectory and are obtained by applying Stokes's theorem to the first form $\int\cdots d\tau$. The upper signs are valid for trajectories with counterclockwise direction of motion, while the lower signs are valid for trajectories with clockwise direction of motion.

Continuity conditions at $E=E_c$. As one can see in Fig. 3 the trajectory $E=E_c$ divides the x-y plane into three different regions. Because the probability should be continuous at $E=E_c$ we have

$$W_{\rm I}(E_c-0)=W_{\rm II}(E_c+0)=W_{\rm III}(E_c+0)\ . \tag{3.11}$$

Furthermore, from the conservation of probability we conclude that

$$S_{\rm I}(E_c-0)=S_{\rm II}(E_c+0)+S_{\rm III}(E_c+0)\ , \tag{3.12}$$

where the probability current density $S(E)$ is given by

$$S(E)=-I(E)W(E)-\Theta J(E)W'(E)\ . \tag{3.13}$$

Because $\partial^2 H/\partial x^2+\partial^2 H/\partial y^2$ has no singularity, the following relations for $I(E)$ and $J(E)$ can easily be derived from (3.10):

$$I_{\rm I}(E_c-0)=I_{\rm II}(E_c+0)+I_{\rm III}(E_c+0)\ , \tag{3.14a}$$

$$J_{\rm I}(E_c-0)=J_{\rm II}(E_c+0)+J_{\rm III}(E_c+0)\ . \tag{3.14b}$$

Combining (3.11)–(3.14) leads to

$$J_{\rm I}(E_c-0)W'_{\rm I}(E_c-0)=J_{\rm II}(E_c+0)W'_{\rm II}(E_c+0)+J_{\rm III}(E_c+0)W'_{\rm III}(E_c+0) \tag{3.15}$$

as the final form of the continuity conditions for $W'(E)$.

IV. CALCULATION OF $T(E)$, $I(E)$, AND $J(E)$

In order to handle (3.9), we must first calculate the quantities $T(E)$, $I(E)$, and $J(E)$. Because we do not need the explicit time dependence of $x(t)$ and $y(t)$ we can

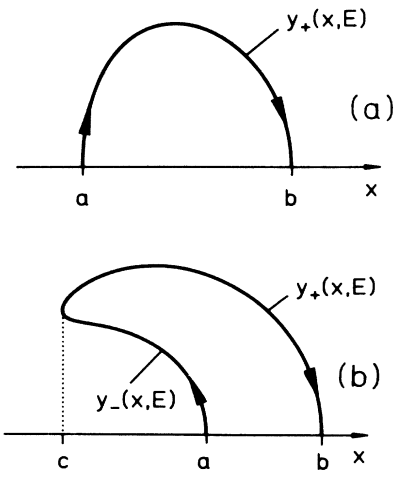

FIG. 4. Possible forms of the trajectories $H(x,y)=E$ for energies where we have only one trajectory $H(x,y)=E$.

make use of energy conservation and obtain from (2.18)

$$y_{\pm}(x,E)=[\tfrac{1}{2}-x^2\pm(\tfrac{1}{4}+2E+2Fx)^{1/2}]^{1/2} \tag{4.1}$$

as an equation for the upper part of the trajectory $H(x,y)=E$. Depending on E, we have only one trajectory or two trajectories $H(x,y)=E$. We first discuss the case that there is only one trajectory $H(x,y)=E$ and then we summarize the changes if there are two trajectories $H(x,y)=E$.

Only one trajectory $H(x,y)=E$ exists. The two possible forms for the trajectory are given in Fig. 4. They are either in region I or in region IIIb. For the trajectory of the form given in Fig. 4(a) the whole upper part of the trajectory (i.e., $y\geq 0$) is given by $y_+(x,E)$ and the direction of motion is clockwise. Therefore we have

$$T(E)=2\int_a^b dx\,(|\dot{x}|)^{-1}\ , \tag{4.2a}$$

$$I(E)=2\int_a^b dx\int_0^{y_+} dy\ , \tag{4.2b}$$

$$J(E)=\int_a^b dx\int_0^{y_+} dy\left[\frac{\partial^2 H}{\partial x^2}+\frac{\partial^2 H}{\partial y^2}\right], \tag{4.2c}$$

where y_+ stands for $y_+(x,E)$. By using (2.17), (2.18), and (4.2) and by making the substitution

$$x=u^2-\frac{1+8E}{8F}\ , \tag{4.3}$$

we arrive at

$$T(E)=\sqrt{2/F}\int_A^B\frac{du}{\sqrt{P_+(u)}}\ , \tag{4.4a}$$

$$I(E)=4\int_A^B\sqrt{P_+(u)}u\,du\ , \tag{4.4b}$$

$$J(E)=\tfrac{4}{3}\int_A^B[3+12\sqrt{2F}u-8P_+(u)]\sqrt{P_+(u)}u\,du\ . \tag{4.4c}$$

The polynomials $P_{\pm}(u)$ are given by

$$P_{\pm}(u)=-\left[u^2-\frac{1+8E}{8F}\right]^2\pm\sqrt{2F}u+\tfrac{1}{2}\ . \tag{4.5}$$

The polynomial $P_-(u)$ has not yet occurred but will appear in our further discussion. The upper and the lower bound of integration are transformed to

$$A=\left[a+\frac{1+8E}{8F}\right]^{1/2},\quad B=\left[b+\frac{1+8E}{8F}\right]^{1/2}. \tag{4.6}$$

If the trajectory looks like the one in Fig. 4(b) the integrals in (4.2) split into two parts and have the form

$$\int_c^a\cdots+\int_c^b\cdots\ , \tag{4.7}$$

where in the first integral $y_-(x,E)$ occurs instead of $y_+(x,E)$ [$P_-(u)$ instead of $P_+(u)$ after the substitution (4.3)]. After some calculations and by using $P_-(-u)=P_+(u)$ we obtain (4.4) with $-A$ instead of A as lower bound of integration. The integration boundaries a and b are the points where the trajectory $H(x,y)$ crosses the x axis. Therefore a and b may be defined by $y_+(a,E)=y_+(b,E)=0$ for trajectories of the form given in Fig. 4(a) and by $y_-(a,E)=y_+(b,E)=0$ for trajectories of the form given in Fig. 4(b). For trajectories of the form of Fig. 4(a) we have

$$P_+(A)=y_+^2(a,E)=0,\quad P_+(B)=y_+^2(b,E)=0\ , \tag{4.8}$$

and for trajectories of the form given in Fig. 4(b) we have

$$\begin{aligned}&P_+(-A)=P_-(A)=y_-^2(a,E)=0\ ,\\ &P_+(B)=y_+^2(b,E)=0\ .\end{aligned} \tag{4.9}$$

It can be shown that $P_+(u)$ cannot have further real zeros if there is only one trajectory $H(x,y)=E$. The determination of the boundaries in the integrals occurring in (4.4) can be simplified by determining the zeros of $P_+(u)$ instead of solving $H(x,0)=E$. Because of (4.8) and (4.9) the results for $T(E)$, $I(E)$, and $J(E)$ given in (4.4) are valid for both forms of trajectories if in (4.4) the smaller of the two real zeros of $P_+(u)$ is used as the lower bound of integration and the larger one is used as the upper bound of integration.

Two trajectories $H(x,y)=E$ exist. The two possible forms of trajectories are shown in Fig. 5. They are either in region II (inner trajectory) or in region IIIa (outer trajectory). The outer trajectory is described by $y_+(x,E)$ [see Fig. 5(a)] or by $y_+(x,E)$ and $y_-(x,E)$ [see Fig. 5(b)]. This is the same as for the case of only one trajectory $H(x,y)=E$. Therefore the results for the outer trajectory are again given by (4.4) if the integration boundaries are chosen properly. The inner trajectory is described by $y_-(x,E)$. In contrast to the outer trajectory, however, the direction of motion is counterclockwise. By similar calculations as done above for the case of a single trajectory $H(x,y)=E$ and by using $P_-(-u)=P_+(u)$ after substituting u by $-u$, we again obtain (4.4). As for the outer trajectory the boundaries for the integrals change and must be specified.

Integration boundaries. As already shown the region of

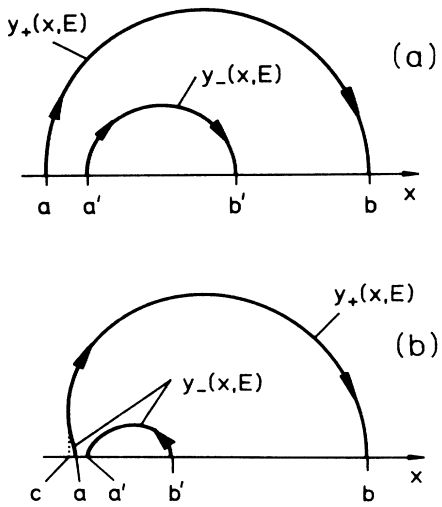

FIG. 5. Possible forms of the trajectories $H(x,y)=E$ for energies where we have two trajectories $H(x,y)=E$.

integration in (4.4) is between the two real zeros of $P_+(u)$ if there is only one trajectory $H(x,y)=E$. If there are two trajectories $H(x,y)=E$ one can easily show that the polynomial $P_+(u)$ has four real zeros. Furthermore, it turns out that one has to integrate (4.4) between the two greatest zeros of $P_+(u)$ if one wants to calculate $T(E)$, $I(E)$, and $J(E)$ for the outer trajectory, whereas (4.4) has to be integrated between the smallest two zeros of $P_+(u)$ if $T(E)$, $I(E)$, and $J(E)$ have to be determined for the inner trajectory.

The polynomial $P_+(u)$ is a polynomial of degree four and the integrands in (4.4) are rational functions of u and $\sqrt{P_+(u)}$. Furthermore, the integration boundaries are zeros of the polynomial $P_+(u)$. Therefore all the integrals occurring in (4.4) can be expressed in terms of the three complete elliptic integrals defined as follows:

$$F\left[\frac{\pi}{2},k\right]=\int_0^{\pi/2}\frac{d\psi}{(1-k^2\sin^2\psi)^{1/2}}\ , \tag{4.10a}$$

$$E\left[\frac{\pi}{2},k\right]=\int_0^{\pi/2}(1-k^2\sin^2\psi)^{1/2}d\psi\ , \tag{4.10b}$$

$$\Pi\left[\frac{\pi}{2},\rho,k\right]=\int_0^{\pi/2}\frac{d\psi}{(1+\rho\sin^2\psi)(1-k^2\sin^2\psi)^{1/2}}\ . \tag{4.10c}$$

The integrals (4.4) are reduced to (4.10a)–(4.10c) by using Refs. 17 and 18. The calculations are lengthy but straightforward. For the results given below we use the abbreviations a_0, a_1, and a_2 defined by

$$\begin{aligned}P_+(u)&=-\left[u^2-\frac{1+8E}{8F}\right]^2+\sqrt{2F}u+\tfrac{1}{2}\\&=-u^4+a_2u^2+a_1u+a_0\ .\end{aligned} \tag{4.11}$$

If $P_+(u)$ has two real zeros, i.e., if $T(E)$, $I(E)$, and $J(E)$ are calculated for the region I or IIIb, we define u_1, u_2, r, s, and k by

$$P_+(u)=-(u-u_1)(u-u_2)[(u-r)^2+s^2],\quad u_1<u_2 \tag{4.12a}$$

$$p=[(u_1-r)^2+s^2]^{1/2}\ , \tag{4.12b}$$

$$q=[(u_2-r)^2+s^2]^{1/2}\ , \tag{4.12c}$$

$$k=\frac{1}{2}\left[\frac{(u_1-u_2)^2-(p-q)^2}{pq}\right]^{1/2}\ . \tag{4.12d}$$

Furthermore, we have

$$I_0=\int_{u_1}^{u_2}\frac{du}{\sqrt{P_+(u)}}=\frac{2}{\sqrt{pq}}F\left[\frac{\pi}{2},k\right]\ , \tag{4.13a}$$

$$I_1=\int_{u_1}^{u_2}\frac{u\,du}{\sqrt{P_+(u)}}=\frac{1}{\sqrt{pq}\,(p-q)}\left[2(pu_2-qu_1)F\left[\frac{\pi}{2},k\right]-(u_2-u_1)(p+q)\Pi\left[\frac{\pi}{2},\frac{(p-q)^2}{4pq},k\right]\right]\ , \tag{4.13b}$$

$$I_2=\int_{u_1}^{u_2}\frac{u^2du}{\sqrt{P_+(u)}}=\frac{2(pu_2^2-qu_1^2)}{\sqrt{pq}\,(p-q)}F\left[\frac{\pi}{2},k\right]+2\sqrt{pq}\,E\left[\frac{\pi}{2},k\right]\ . \tag{4.13c}$$

If $P_+(u)$ has four real zeros, i.e., if $T(E)$, $I(E)$, and $J(E)$ are calculated for the regions II and IIIa, we define u_1, u_2, u_3, u_4, Δ, and k by

$$P_+(u)=-(u-u_1)(u-u_2)(u-u_3)(u-u_4)\ , \qquad u_1<u_2<u_3<u_4 \tag{4.14a}$$

$$\Delta=[(u_4-u_2)(u_3-u_1)]^{1/2}\ , \tag{4.14b}$$

$$k=\left[\frac{(u_4-u_3)(u_2-u_1)}{(u_4-u_2)(u_3-u_1)}\right]^{1/2}\ . \tag{4.14c}$$

Instead of (4.13) we use the integrals

$$I_0=\int_{u_3}^{u_4}\frac{du}{\sqrt{P_+(u)}}=\frac{2}{\Delta}F\left[\frac{\pi}{2},k\right]\ , \tag{4.15a}$$

$$\begin{aligned}I_1&=\int_{u_3}^{u_4}\frac{u\,du}{\sqrt{P_+(u)}}\\&=\frac{2}{\Delta}\left[u_1F\left[\frac{\pi}{2},k\right]+(u_4-u_1)\Pi\left[\frac{\pi}{2},\frac{u_4-u_3}{u_3-u_1},k\right]\right]\ ,\end{aligned} \tag{4.15b}$$

$$\begin{aligned}I_2&=\int_{u_3}^{u_4}\frac{u^2du}{\sqrt{P_+(u)}}\\&=\Delta E\left[\frac{\pi}{2},k\right]-\frac{u_1u_2+u_3u_4}{\Delta}F\left[\frac{\pi}{2},k\right]\ .\end{aligned} \tag{4.15c}$$

If we furthermore define for both cases

$$J_1=\tfrac{3}{8}a_1I_2+(\tfrac{1}{2}a_0+\tfrac{1}{8}a_2^2)I_1+\tfrac{1}{16}a_1a_2I_0\ , \tag{4.16a}$$

$$J_2=(\tfrac{2}{5}a_0+\tfrac{2}{15}a_2^2)I_2+\tfrac{1}{4}a_1a_2I_1+(\tfrac{3}{40}a_1^2+\tfrac{1}{15}a_0a_2)I_0\ , \tag{4.16b}$$

$$\begin{aligned}J_3=&(\tfrac{113}{640}a_1a_2^2+\tfrac{81}{160}a_0a_1)I_2\\&+(\tfrac{3}{16}a_0a_2^2+\tfrac{3}{16}a_1^2a_2+\tfrac{3}{128}a_2^4+\tfrac{3}{8}a_0^2)I_1\\&+(\tfrac{47}{320}a_0a_1a_2+\tfrac{27}{640}a_1^3+\tfrac{3}{256}a_1a_2^3)I_0\ ,\end{aligned} \tag{4.16c}$$

the results for the regions I and III can be written as

$$T(E)=\sqrt{2/F}I_0\ , \tag{4.17a}$$

$$I(E)=4J_1\ , \tag{4.17b}$$

$$J(E)=4J_1+16\sqrt{2F}J_2-\tfrac{32}{3}J_3\ . \tag{4.17c}$$

If in (4.15) the region of integration is between u_1 and u_2, the results for I_0 and I_2 do not change, whereas I_1 becomes the original I_1 (obtained with the boundaries u_3 and u_4) minus π. Therefore (4.17) is valid for region II if in (4.16) I_1 is replaced by $I_1-\pi$.

For numerical calculations the derivatives of $I(E)$ and $J(E)$, denoted by $I'(E)$ and $J'(E)$, respectively, are also useful. By using the second part of (3.10a), transforming it to the variables E and τ, and taking the derivative with respect to E, it can be shown that $I'(E)$ is identical to $T(E)$. The derivative of J, i.e, $J'(E)$, cannot be expressed by $T(E)$, $I(E)$, or $J(E)$. It is given by

$$J'(E)=\sqrt{2/F}I_0+8I_1=T(E)+8I_1 \ . \tag{4.18}$$

Again the result is valid for the regions I and III and applies also to the region II if I_1 is replaced by $I_1-\pi$.

The functions $T(E)$, $I(E)$, $J(E)$, and $J'(E)$ are shown in Fig. 6. At $E=E_c$, both $T(E)$ and $J'(E)$ have a logarithmic singularity, which does not appear as a singularity but as a peak.

In the vicinity of the minimum of $H(x,y)$ ($E=E_0$, region I) or in the vicinity of the maximum of $H(x,y)$ ($E=E_1$, region II) the trajectories remain in the vicinity of the minimum or the maximum of $H(x,y)$. Therefore $H(x,y)$ can be expanded around its minimum and its maximum up to second order in x and y. The corresponding equation for the undamped motion is linear and can easily be solved yielding

$$T(E)\approx\frac{2\pi}{[H_{xx}(\hat{x},0)H_{yy}(\hat{x},0)]^{1/2}} \ , \tag{4.19a}$$

$$I(E)\approx T(\hat{E})(E-\hat{E})$$
$$\approx\frac{2\pi(E-\hat{E})}{[H_{xx}(\hat{x},0)H_{yy}(\hat{x},0)]^{1/2}} \ , \tag{4.19b}$$

$$J(E)\approx\tfrac{1}{2}[H_{xx}(\hat{x},0)+H_{yy}(\hat{x},0)]I(E)$$
$$\approx\frac{\pi[H_{xx}(\hat{x},0)+H_{yy}(\hat{x},0)](E-\hat{E})}{[H_{xx}(\hat{x},0)H_{yy}(\hat{x},0)]^{1/2}} \ , \tag{4.19c}$$

$$J'(E)\approx\tfrac{1}{2}[H_{xx}(\hat{x},0)+H_{yy}(\hat{x},0)]T(E)$$
$$\approx\frac{\pi[H_{xx}(\hat{x},0)+H_{yy}(\hat{x},0)]}{[H_{xx}(\hat{x},0)H_{yy}(\hat{x},0)]^{1/2}} \ , \tag{4.19d}$$

as an approximation valid for $E\approx\hat{E}$. In (4.19), $\hat{E}$ stands for either E_0 or E_1. Because of the symmetry of $H(x,y)$ the point (x,y), where H has its minimum or its maximum lies on the x axis, i.e., at $y=0$. The corresponding x value is denoted by $\hat{x}$ and stands for both x_0 and x_1. [$H(x,y)$ has its minimum E_0 at $x=x_0$, $y=0$ and its maximum E_1 at $x=x_1$, $y=0$.] Furthermore, H_{xx} and H_{yy} are given by

$$H_{xx}=\frac{\partial^2 H}{\partial x^2}, \quad H_{yy}=\frac{\partial^2 H}{\partial y^2} \ . \tag{4.20}$$

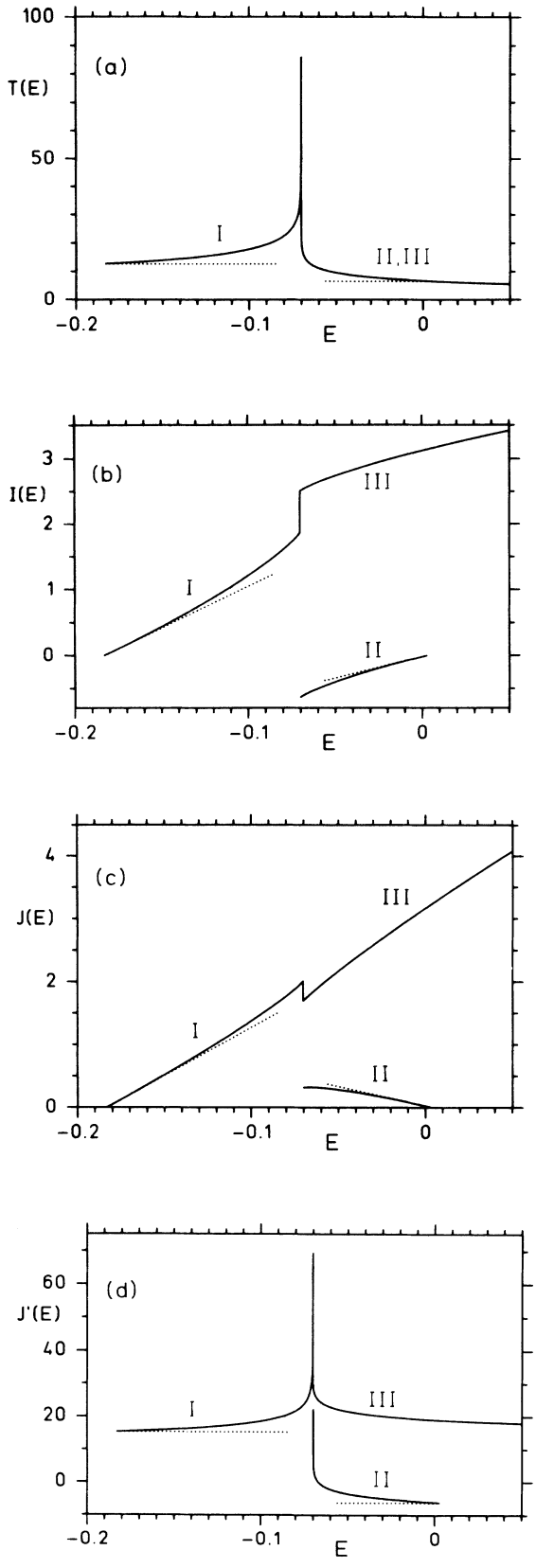

FIG. 6. The functions (a) $T(E)$, (b) $I(E)$, (c) $J(E)$, and (d) $J'(E)$ for $F=0.08$. The peaks in (a) and (d) are logarithmic singularities. The dotted lines are the approximations (4.19).

V. NUMERICAL DETERMINATION OF THE EIGENVALUES

Because we are only interested in the long-time behavior of (3.9) we do not need the full time-dependent solution and insert the ansatz

$$W(E,t)=e^{-2\gamma\lambda t}\phi(E) \tag{5.1}$$

into (3.9). If the eigenvalue λ is well separated from the higher ones, it describes the long-time behavior of the system. After some algebra and by using $I'(E)=T(E)$ we arrive at the eigenvalue equation

$$\Theta J(E)\phi''(E)+[I(E)+\Theta J'(E)]\phi'(E)+(\lambda+1)T(E)\phi(E)=0 . \tag{5.2}$$

The boundary condition for (5.2) is

$$\phi(E)\to 0 \quad \text{for } E\to\infty . \tag{5.3}$$

Because there is no singularity at $E=E_0$ or at $E=E_1$ and because $I(E)$ and $J(E)$ vanish at $E=E_0$ and at $E=E_1$ [see the second form of (3.10); the area enclosed by the trajectory becomes zero for $E\to E_0,E_1$] we conclude from (5.2)

$$\phi'(\hat{E})=-\frac{2(\lambda+1)\phi(\hat{E})}{\Theta[H_{xx}(\hat{x},0)+H_{yy}(\hat{x},0)]} \quad \text{for } \hat{E}=E_0,E_1,\ \hat{x}=x_0,x_1 , \tag{5.4}$$

where we have used (4.19a)–(4.19d). The procedure for solving (5.2) numerically is a modified shooting method.[19] The various steps are as follows.

(1) Choose an approximate value for λ.

(2) Integrate (5.2) in the regions I and II starting at $E=E_0$ and $E=E_1$, respectively, and end at $E=E_c$. The initial conditions for $\phi(E)$ are arbitrary, the initial conditions for $\phi'(E)$ follow from (5.4).

(3) Scale $\phi_{\rm I}(E)$ and $\phi_{\rm II}(E)$ such that $\phi_{\rm I}(E_c)=\phi_{\rm II}(E_c)$.

(4) Integrate (5.2) in the region III starting at $E=E_c$. The initial conditions for $\phi(E)$ and $\phi'(E)$ follow from the continuity conditions for $\phi(E)$ and $\phi'(E)$ at $E=E_c$; see (3.11) and (3.15). The upper limit for the integration is some large value $E_{\rm max}$ on which the result must not depend.

(5) Determine λ such that $\phi(E_{\rm max})=0$ by a root-finding technique such as *regula falsi*, for instance.

(6) Normalize the result for $\phi(E)$ if necessary (not necessary for determining the eigenvalue only).

VI. APPROXIMATION FOR SMALL Θ

In this section we show how the one-dimensional Fokker-Planck equation (3.9) can be solved approximately if the normalized temperature Θ as defined in (2.13) is small compared to 1. As explained in Sec. II we still have to require that the thermal energy kT must be large compared to the photon energy $\hbar\omega_c$. The combination of these two conditions leads to

$$1\ll\frac{kT}{\hbar\omega_c}\ll\frac{\Omega}{\chi} . \tag{6.1}$$

For suitable parameters such a condition can still be fulfilled. In order to obtain an approximate result for the lowest nonzero eigenvalue we substitute the ansatz (5.1) into (3.9). By integrating the resulting equation we obtain for regions I and II the integral-differential equation

$$I(E)\phi(E)+\Theta J(E)\phi'(E)=-\lambda\int_{\hat{E}}^{E}T(E')\phi(E')dE' . \tag{6.2}$$

Here $\hat{E}$ stands for E_0 if region I is investigated, whereas for region II we have $\hat{E}=E_1$. The contribution from the lower bound $\hat{E}$ to the left-hand side of (6.2) vanishes because of $I(\hat{E})=J(\hat{E})=0$. (For a transformation of the Fokker-Planck equation in the overdamped case to the Fredholm integral equation and for a discussion for obtaining the lowest nonzero eigenvalue from the equation see Sec. 5.10.2 of Ref. 20. The same procedure can also be applied to the underdamped case.) If the term on the right-hand side of (6.2) is interpreted as an inhomogeneity of a linear first-order differential equation the solution of the "differential equation" (6.2) is given by

$$\phi(E)=\phi(E_c)e^{[g(E_c)-g(E)]/\Theta}-\frac{\lambda}{\Theta}e^{-g(E)/\Theta}\int_{E_c}^{E}dE'\frac{e^{g(E')/\Theta}}{J(E')}\times\int_{\hat{E}}^{E'}T(E'')\phi(E'')dE'' , \tag{6.3}$$

where the function $g(E)$ is defined by

$$g(E)=\int_{\hat{E}}^{E}\frac{I(E')}{J(E')}dE' . \tag{6.4}$$

The probability current density in regions I and II reads

$$S(E)=-I(E)\phi(E)-\Theta J(E)\phi'(E)=\lambda\int_{\hat{E}}^{E}T(E')\phi(E')dE' . \tag{6.5}$$

If λ is small, $\phi(E)$ approximately obeys the equation for the stationary solution, i.e.,

$$\left[I(E)+\Theta J(E)\frac{d}{dE}\right]\phi(E)\approx\text{const}=0 . \tag{6.6}$$

Because $I(\hat{E})=J(\hat{E})=0$ and because $\phi(E)$ and $\phi'(E)$ do not have any singularity at $E=\hat{E}$, the constant in the above equation must be equal to zero. Therefore we have in regions I and II as well as in region III

$$\phi(E)\approx Ae^{-g(E)/\Theta} . \tag{6.7}$$

Substituting this expression into the integrals leads to

$$\int_{\hat{E}}^{E}T(E')\phi(E')dE'\approx A\int_{\hat{E}}^{E}T(E')e^{-g(E')/\Theta}dE'=A\int_{\hat{E}}^{E}T(E')\frac{J(E')}{I(E')}g'(E')e^{-g(E')/\Theta}dE' . \tag{6.8}$$

Because $\exp[-g(E)/\Theta]$ vanishes rapidly if $E\neq\hat{E}$ (Θ small) we obtain

$$\int_{\hat{E}}^{E} T(E')\phi(E')dE'$$
$$\approx AT(\hat{E})\frac{J'(\hat{E})}{I'(\hat{E})}\int_{\hat{E}}^{E} g'(E')e^{-g(E')/\Theta}dE'$$
$$\approx A\Theta J'(\hat{E}) , \tag{6.9}$$

where we have used l'Hospital's rule for the expression

$$\lim_{E\to\hat{E}}\frac{J(E)}{I(E)}=\frac{J'(\hat{E})}{I'(\hat{E})}=\frac{J'(\hat{E})}{T(\hat{E})} . \tag{6.10}$$

Substituting (6.9) into (6.5) the probability current density becomes

$$S(E)\approx\lambda\Theta AJ'(\hat{E}) , \tag{6.11}$$

which is valid in regions I and II if E is not too close to the extremal value $\hat{E}$ (the term $\exp[-g(E)/\Theta]$ has been neglected in (6.9)). From (6.3) and (6.9) we obtain

$$\phi(E)\approx\phi(E_c)e^{[g(E_c)-g(E)]/\Theta}$$
$$-\lambda AJ'(\hat{E})e^{-g(E)/\Theta}\int_{E_c}^{E}\frac{e^{g(E')/\Theta}}{J(E')}dE' . \tag{6.12}$$

The main contribution to the above integral stems from the region $E\approx E_c$ because $\exp[g(E)/\Theta]$ becomes very large at $E=E_c$. Therefore the integral can be approximated by

$$\int_{E_c}^{E}\frac{e^{g(E')/\Theta}}{J(E')}dE'=\int_{E_c}^{E}\frac{g'(E')e^{g(E')/\Theta}}{I(E')}dE'$$
$$\approx\frac{1}{I(E_c)}\int_{E_c}^{E}g'(E')e^{g(E')/\Theta}dE'$$
$$\approx-\frac{\Theta}{I(E_c)}e^{g(E_c)/\Theta} . \tag{6.13}$$

Substituting (6.13) into (6.12) leads to the approximation

$$\phi(E)\approx\left[\phi(E_c)+\lambda\Theta A\frac{J'(\hat{E})}{I(E_c)}\right]e^{[g(E_c)-g(E)]/\Theta} \tag{6.14}$$

for $\phi(E)$ valid in regions I and II if E is not too close to $\hat{E}$ or E_c. Because (6.14) and (6.7) must agree (at least approximately) we conclude that the constant A must be given by

$$A=\frac{\phi(E_c)}{e^{-g(E_c)/\Theta}-\lambda\Theta J'(\hat{E})/I(E_c)} . \tag{6.15}$$

Therefore the probability current density reads

$$S(E)=\frac{\lambda\Theta J'(\hat{E})\phi(E_c)}{e^{-g(E_c)/\Theta}-\lambda\Theta J'(\hat{E})/I(E_c)} . \tag{6.16}$$

In region III we obtain instead of (6.5)

$$S(E_c)=-\lambda\int_{E_c}^{\infty}T(E')\phi(E')dE'$$
$$=\lambda I(E_c)\phi(E_c)+\lambda\int_{E_c}^{\infty}I(E')\phi'(E')dE'$$
$$\approx\lambda I(E_c)\phi(E_c)+\lambda I(E_c)\int_{E_c}^{\infty}\phi'(E')dE'=0 ,$$

(6.17)

if the region of integration is between E_c and infinity. In (6.17) we have used $S(\infty)=0$ and the fact that $\phi'(E)$ vanishes rapidly if E is not close to E_c. [$\phi(E)$ may again be approximated by (6.7) if Θ is small.] A partial integration was necessary because of $T(E)\to\infty$ for $E\to E_c$. The continuity conditions at $E=E_c$ are

$$\phi_{\rm I}(E_c-0)=\phi_{\rm II}(E_c+0)=\phi_{\rm III}(E_c+0)=\phi(E_c) , \tag{6.18a}$$

$$S_{\rm I}(E_c-0)=S_{\rm II}(E_c+0) . \tag{6.18b}$$

Form (6.16) and the continuity conditions (6.18) one can easily conclude that the eigenvalue λ is given by

$$\lambda=\frac{1}{\Theta}\frac{I_{\rm I}(E_c-0)I_{\rm II}(E_c+0)}{I_{\rm II}(E_c+0)-I_{\rm I}(E_c-0)}$$
$$\times\left[\frac{e^{-g_{\rm I}(E_c-0)/\Theta}}{J'_{\rm I}(E_0)}-\frac{e^{-g_{\rm II}(E_c+0)/\Theta}}{J'_{\rm II}(E_1)}\right] . \tag{6.19}$$

For simplicity $J'_{\rm I}(E_0)$ and $J'_{\rm II}(E_1)$ can be expressed by the second derivatives of H as given in (4.19d). In order to obtain transitions from E_0 to E_1 and vice versa the solution of the Langevin equations (2.15) has to cross the critical trajectory $H(x,y)=E_c$. Obviously, (6.19) is the sum of two terms [$J'_{\rm I}(E_1)$ is negative; see Fig. 6(c)]. The first term may be interpreted as the transition from the minimum E_0 of $H(x,y)$ over the trajectory $H(x,y)=E_c$. The second term describes the transition from the max-

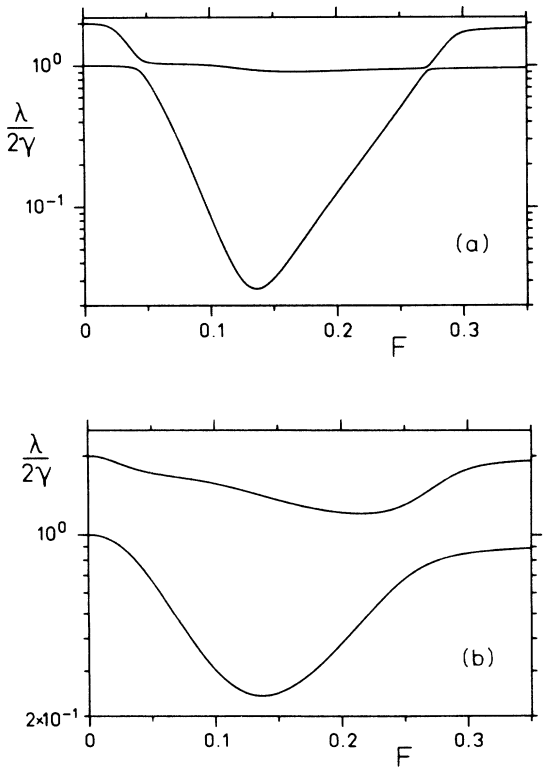

FIG. 7. The first two nonvanishing eigenvalues of the classical Fokker-Planck equation (2.12) as a function of the driving field F for $\gamma=0.1$. The values for Θ are (a) 0.02 and (b) 0.05.

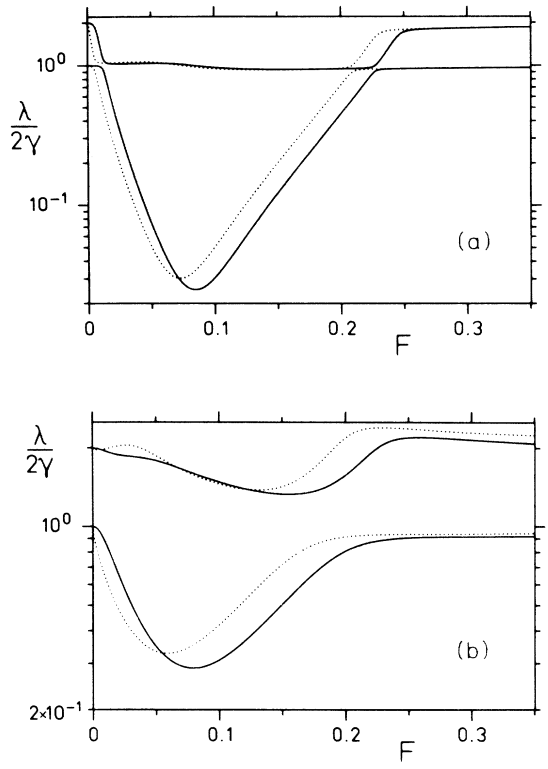

FIG. 8. The first two nonvanishing eigenvalues of the classical Fokker-Planck equation (2.12) as a function of the driving field F for $\gamma=0.01$. The values for Θ are (a) 0.02 and (b) 0.05. The dotted lines are the eigenvalues of (3.9) (approximation for small cavity damping).

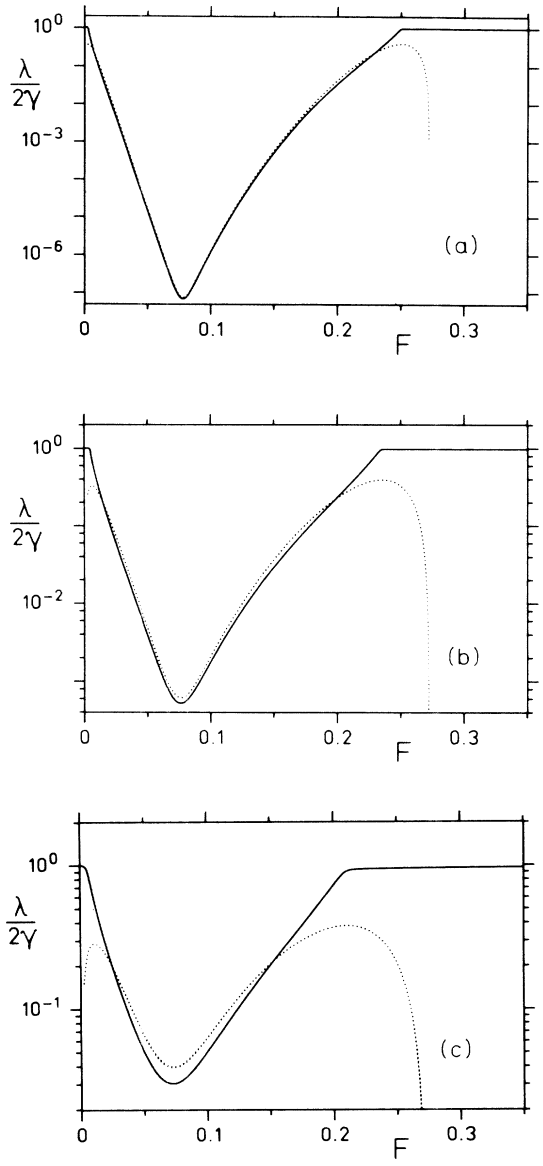

FIG. 9. The first nonvanishing eigenvalue of (3.9) (approximation for small cavity damping) for (a) $\Theta=0.005$, (b) 0.01, and (c) 0.02. The dotted lines follow from (6.19) (approximation for small cavity damping and small Θ).

imum E_1 of $H(x,y)$ over the trajectory $H(x,y)=E_c$. The functions $g_{\rm I}(E_c-0)$ and $g_{\rm II}(E_c+0)$ correspond to the barrier heights of the potential in the Kramers problem. Similar but simpler calculations have been applied to the Brownian motion of a particle in a bistable potential; see, for instance, Ref. 5. For low Θ and small damping one obtains instead of (6.19) the well-known result of Kramers;[21] see also Ref. 5. Thus (6.19) is the Kramers's escape rate applied to the more complicated Hamilton function (2.18).

VII. NUMERICAL RESULTS

In Ref. 3 the exact equation of motion for the quasiprobability distribution as a Fokker-Planck approximation were solved numerically by using the matrix continued-fraction method. With

$$\alpha=z,\quad \alpha^*=z^*,\quad \Omega=-1,\quad \chi=1,\quad \kappa=\gamma\ ,\qquad 2n_{\rm th}+1=4\Theta\ , \tag{7.1}$$

the Fokker-Planck operator (4.8) of Ref. 3 exactly agrees with the Fokker-Planck operator of our classical equation (2.12). Therefore we can obtain exact eigenvalues of the classical equation (2.12) by using the matrix continued-fraction method as described in Refs. 2 and 3. The results are shown in Fig. 7. As one expects the first nonvanishing eigenvalue is small for such F values where the system is bistable. If the temperature is increased the transition rate as well as the first nonvanishing eigenvalue must become larger. This behavior is clearly visible in Figs. 7 and 8. Because of convergence problems it becomes more and more time-consuming to determine the exact eigenvalues for small cavity damping by using matrix continued fractions. For $\gamma=0.01$ and $\Theta=0.02$ [Fig. 8(a)] we were able to calculate eigenvalues with double precision arithmetic. For smaller γ or Θ the matrix continued-fraction method needs a higher precision arithmetic.

In Fig. 8 the approximation for small cavity damping described in Secs. II–IV is compared to the exact solution. As one can see the shapes are almost the same.

However, the approximate curve is shifted a bit to the left compared with the exact solution. The deviations for the same F are of the order of 30% for the lowest nonvanishing eigenvalue. It seems that $\gamma=0.01$ is not low enough for a precise agreement with the zero-friction-limit result. In analogy to the Brownian motion problem in a bistable potential, one expects that in the limit $\gamma\to 0$ the ratio $\lambda/(2\gamma)$ is a linear function of $\sqrt{\gamma}$ for small damping; see Refs. 5 and 22–24. Therefore the deviations are of the order $\sqrt{\gamma}\approx 0.1$ in agreement with Fig. 8(a).

In Fig. 9 the approximation for small cavity damping and small Θ (6.19) is compared with the first nonvanishing eigenvalue determined numerically from the one-variable Fokker-Planck equation (3.9) (approximation for small cavity damping). It can be seen that the agreement is good in the bistable region, especially for low normalized temperatures Θ. It should be mentioned, however, that even in the limit $\Theta\to 0$ the approximation fails at $F\approx 0.27$. This can be explained as follows: For $F>2/(3\sqrt{6})\approx 0.272\,16\ldots$ there is only one trajectory $H(x,y)$ for any value of E, i.e., the topology given in Fig. 1 is no longer valid. Because this topology was essential for the derivation of (6.19) the result (6.19) cannot be valid for $F>2/(3\sqrt{6})$.

VIII. SUMMARY

We have shown that in the limit of large photon numbers the equation of motion for the quasiprobability distribution describing dispersive optical bistability reduces to an ordinary two-variable Fokker-Planck equation. This equation, which does not fulfill the condition of detailed balance, can be solved by the matrix continued-fraction method. For small cavity damping the energy becomes a slow variable. In the limit $\gamma\to 0$ one obtains a one-variable Fokker-Planck equation, which was solved numerically by a shooting method. It agrees quite well with the result of the matrix continued-fraction method. If, in addition, the number of thermal photons is small compared to the number of photons inside the cavity, an analytic expression for the lowest nonzero eigenvalue was obtained in analogy to the Brownian motion problem for small damping. In particular, the lowest nonzero eigenvalue was determined, which describes the transition rate between the bistable states.

[1]P. Drummond and D. F. Walls, J. Phys. A **13**, 725 (1980).
[2]K. Vogel and H. Risken, Phys. Rev. A **38**, 2409 (1988).
[3]K. Vogel and H. Risken, Phys. Rev. A **39**, 4675 (1989).
[4]K. E. Cahill and R. J. Glauber, Phys. Rev. **177**, 1882 (1969).
[5]H. Risken and K. Voigtlaender, J. Stat. Phys. **41**, 825 (1985).
[6]H. Risken, C. Savage, F. Haake, and D. F. Walls, Phys. Rev. A **35**, 1729 (1987).
[7]H. Risken and K. Vogel, Phys. Rev. A **38**, 1349 (1988).
[8]K. Vogel, Ph.D. thesis, Universität Ulm, Federal Republic of Germany, 1989.
[9]M. I. Dykman and V. N. Smelyanskii, Zh. Eksp. Teor. Fiz. **94**, 61 (1988) [Sov. Phys.—JETP **67**, 1769 (1989)].
[10]H. Haug, S. W. Koch, R. Neumann, and H. E. Schmidt, Z. Phys. B **49**, 79 (1982).
[11]R. Graham and A. Schenzle, Phys. Rev. A **23**, 1302 (1981).
[12]P. D. Drummond, Phys. Rev. A **33**, 4462 (1986).
[13]P. Filipowicz, J. C. Garrison, P. Meystre, and E. M. Wright, Phys. Rev. A **35**, 1172 (1987).
[14]G. Duffing, *Erzwungene Schwingungen bei Veränderlicher Eigenfrequenz und ihre Technische Bedeutung* (Vieweg, Braunschweig, 1918).
[15]A. H. Nayfeh and D. T. Mook, *Nonlinear Oscillations* (Wiley, New York, 1979), p. 162ff.
[16]R. L. Stratonovich, *Topics in the Theory of Random Noise* (Gordon and Breach, New York, 1967), Vols. I and II.
[17]I. S. Gradshteyn and I. M. Ryzhik, *Table of Integrals, Series, and Products*, 4th ed. (Academic, New York, 1965).
[18]W. Gröbner and N. Hofreiter, *Integraltafel, Erster Teil*, 5th ed. (Springer, Wien, 1975).
[19]W. H. Press, B. P. Flannery, S. A. Teukolsky, W. T. Vettering, *Numerical Recipes* (Cambridge University Press, Cambridge, 1986).
[20]H. Risken, *The Fokker-Planck Equation* (Springer, Berlin, 1989).
[21]H. A. Kramers, Physica **7**, 284 (1940).
[22]M. Büttiker and R. Landauer, Phys. Rev. B **30**, 1551 (1984).
[23]V. I. Mel'nikov and S. V. Meshkov, J. Chem. Phys. **85**, 1018 (1986).
[24]H. Risken, K. Vogel, H. D. Vollmer, IBM J. Res. Dev. **32**, 112 (1988).